Int. J. Electrochem. Sci., 8 **(2013)** 535 - 547

International Journal of
ELECTROCHEMICAL
SCIENCE
www.electrochemsci.org

Characterization of Phosphoric Acid Doped N-type Silicon Thin Films Printed on ITO Coated PET Substrate

M. K. M. Ali[1,*], *K. Ibrahim*[1], *E.M. Mkawi*[1] *and A. Salhin*[2]

[1] Nano-Optoelectronics Research and Technology Laboratory, School of Physics, Universiti Sains Malaysia, 11800 Penang, Malaysia
[2] School of Chemical Sains, Universiti Sains Malaysia, Penang 11800, Malaysia
[*]E-mail: hamofarog@yahoo.com

Received: 16 October 2012 / *Accepted:* 30 November 2012 / *Published:* 1 January 2013

In this paper n-type polycrystalline silicon thin films deposited on ITO coated polyethylene terephthalate (PET) substrate by screen printing technique have been studied. The phosphoric acid with different concentration used as doping source to create n-type silicon powder which is dissolved in solvent to obtain n- type silicon pastes have three different doping concentration and constant viscosity . These pastes used to print n-type polycrystalline silicon thin films with thicknesses of 611± 8 nm for etch and different phosphorus doping concentrations. Among the techniques applied to analyze the properties of poly-Si thin layers to evaluate the effect doping variation. X-ray diffraction (XRD) technique was used for the determination of the crystallites size (*D*) and the stress in poly-Si thin films. The surface morphology and roughness carried out by Scanning electron microscopy (SEM) and atomic force microscopy (AFM). Thin film components elements detected by (EDX) attached with SEM system. The electrical properties such as resistivity, carrier concentration and Hall mobility were carried out by Hall Effect measurements. Optical transmittance and the transmittance ratio and others optical properties of the films are reported. Details on the sample preparations and experimental details will be presented.

Keywords: N-type poly-Si; thin film, screen printing; PET

1. INTRODUCTION

The polycrystalline silicon is considered as good candidates for the active layer of the thin film solar cells and for other large area electronics [1]. Reducing the cost of solar cells fabrication is the main objective of majority photovoltaic researches. This goal can be achieved by using inexpensive substrate and low cost fabrication processes [2-5]. The screen-printing technology currently is well established [6] and the head of these processes. This technique shows various advantages such as low

cost and high productivity which were useful to achieve this current work. The screen printing is relatively new thin-film polycrystalline-silicon solar cell technology aims at low-cost devices with acceptable energy conversion efficiencies. The material is fully crystalline, a few microns thick, supported by an inexpensive non-Si substrate and has a typical grain size in the range of 0.1 to 13 μm can be produced by screen printing technique[7-10] This technology combines the cost reduction potential of a thin-film technology with the good material quality of crystalline Si. Historically, photovoltaic research mainly focused on p-type absorber material. However, n-type material is an attractive alternative. In this research n-type polycrystalline silicon thin films deposited on ITO-coated polyethylene terephthalate (PET) substrate using a screen-printing technique were studied. Phosphoric acid with different concentrations was used as a doping source to create n-type silicon powder which is dissolved in solvent to obtain n-type silicon pastes have three different doping concentrations and constant viscosity. These pastes were used to print n-type polycrystalline silicon thin films with thicknesses of 611 $\pm$ 8 nm for each different phosphorus-doping concentration. In order to study the doping concentration, n-Si films deposited on ITO coated PET substrate with thicknesses of 619 nm, 611 nm and 603 nm doped with phosphoric acid concentrations of 10 grams/liter, 20 grams/liter and 30 grams/liter respectively.

2. EXPERIMENTAL

2.1 Preparation of Phosphor doped silicon powder

This method used phosphoric acid (H_3PO_4) as the doping source and silicon powder to obtain phosphorus doped n-type silicon powder [11-13]. Fine silicon powder is stirred in a diluted solution of phosphoric acid with purity of 97% having different concentrations. The silicon particles in powder are dried with the phosphorus film then the phosphorus driven into the silicon particles. The method of doping comprises the following steps:

a. Preparing a diluted solution of phosphoric acid with different concentrations by dissolving 0.5, 1.0 and 1.5 grams of phosphoric acid in 50 ml of deionized water for each mentioned weight. The obtained phosphoric acid concentrations were 10, 20 and 30 grams/liter respectively.

b. Mixing 5 grams of silicon powder with 20 ml of diluted phosphoric acid with the above-mentioned concentrations.

c. Stirring the solutions for 5 min to coat the silicon particles with different concentrations of the phosphorus compound.

d. The silicon powder was filtered and dried by heating at 100 °C until no solvent remains then butted in soft beck at 120 °C for 15 min.

e. Diffusing the said phosphorus coating phosphorus into the silicon particles by heating to a temperature of approximately 850 -900 °C with a nitrogen flowing rate of 5 sccm for hour.

2.2 N-type silicon paste preparation

To fabricate n-type silicon paste for screen printing, silicon powder with different phosphorus doping concentrations was dissolved in polyethylene glycol organic solvents and the viscosity was adjusted by adding a suitable thinner to the liquid base. Toluene was used as both the original solvent for the polymer and the thinner [12]. N-type silicon paste preparation can be summarized in the following steps:

a. 10 grams of solid polymer polyethylene glycol was dissolved in 40 ml of toluene.

b. To a 250 ml 3-neck flask placed on a hot plate with a mechanical stirrer and a nitrogen inlet/outlet was added 5 grams of phosphorus-doped silicon powder mixed with 20 ml of polyethylene glycol solvent, using the condensation method which is explained in Figure 3.4 The mixture in the condensation system was stirred at 400 round/min at 150 ^{o}C under a nitrogen gas aperture for 4 hours.

c. Step (b) was repeated for the same weight with different doping concentrations of silicon powder to obtain silicon pastes having three different concentrations and fixed viscosity.

d. The viscosity was adjusted by adding toluene to be a constant value for the three different phosphorus doping concentrations.

e. Silicon pastes with three different phosphorus doping concentrations and the same viscosity of 171 Pa·s were used to print 611$\pm$ 8 nm thickness of three n-type polycrystalline silicon thin films on ITO-coated PET substrate.

2.3 Thin Film Preparation:

The substrate was PET sheet, which was degreased ultrasonically in a dilute detergent solution, rinsed in demonized water, and blown dry in N2 gas before they were used.PET substrates were coated by 25 nm of ITO thin film by DC sputtering method. A description of the screen printing process, depicted in Figure 2. The screen is placed a few millimeters above the surface of the PET substrate. Upon loading the silicon pasted solution onto the screen, a rub ‘‘squeegee’’ is then swept with a velocity of several centimeters per second across the surface of the screen, momentarily contacting it to the substrate. At this point, solution flows from the screen to the surface of the PET substrate. As the squeegee then passes over a region, the screen separates from the substrate, leaving behind solution that dries to yield a continuous film. For this study, a screen with area of 40 x40 cm^2 and a mesh count of 181/cm was used.

2.4 Thin Film characterization

In order to study the structural characteristics of the n-type silicon thin films have different doping concentration and small variation in thickness, we have characterized them by different techniques. The effect of phosphor doping concentration on the Si layers structures was evaluated by Raman spectroscopy and Hall Effect measurement in the fixed thickness of silicon thin film. The Viscosities was measured by using Standard spindles of Visco Basic plus Viscometer. The thickness

of the c-Si film was determined by using optical reflectometer (Model: Filmetric F20).. Raman spectroscopy system (model: Jobin Yvon HR 800 UV), has been used to investigate the effect of phosphorus doping concentration on crystallization of Si thin films. The surface morphology of Si films was studied by Atomic Force Microscope (AFM, model: Ultra Objective) and scanning electron microscope (SEM, model: JSM–6460 LV). X-ray diffraction (XRD) measurements were performed using high resolution X-ray diffractometer system (model: P Analytical X' Pert PRO MRD PW3040). Structural changes of the Si films were evaluated by X-ray diffraction (XRD) measurements in the 2θ mode. Carrier concentration and Hall mobility were obtained by Hall-effect measurement system (Model: Accent/HL 5500 PC). The sheet resistance and the resistivity of the film were measured also by Hall-effect measurement. The optical transmittance of the films was measured as the transmittance ratio of a film coated substrate relative to an uncoated substrate by UV Spectrophotometer (Model: U-2000 HITACHI).

3.RESULTS AND DISCUSSIONS

3.1 Raman spectrum of n-type silicon thin films printed on ITO-coated PET

Fig.1shows the Raman spectrums of n-Si films deposited on PET substrate with thicknesses of (a) 619 nm, (b) 611 nm and (c) 603 nm doped with phosphoric acid concentrations of 10 grams/liter, 20 grams/liter and 30 grams/liter respectively .The structure of the film phase composition can be obtained by analysis of the Raman scattering data. A very sharp threshold for crystallization observed for the crystalline silicon (of the transversal optical (TO) phonon peak at ~520 cm^{-1}) was obtained for sample (c) [14].

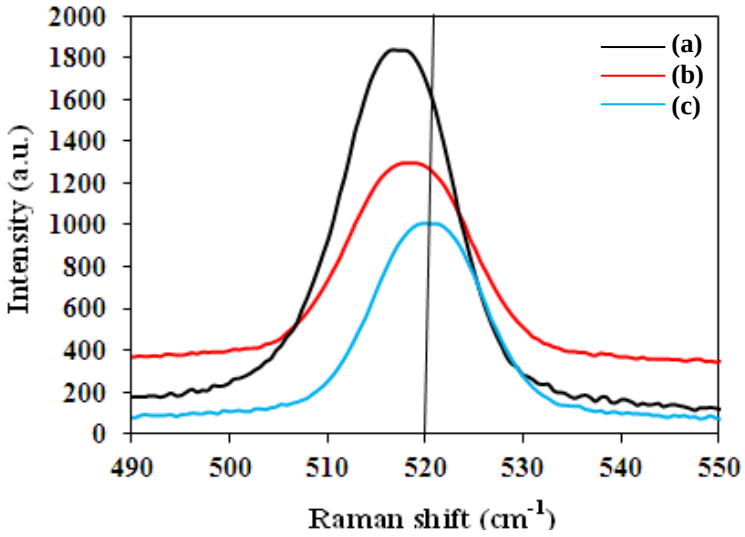

Figure 1. Raman spectrums of on-Si films deposited on PET substrate with thicknesses of (a) 619 nm, (b) 611 and (c) 603 nm doped with phosphoric acid concentrations of 30 grams/liter, 20 grams/liter and 10 grams/liter respectively.

The peak position of the Raman TO-mode shown in Figure 5.18 (c) is shifted to lower wave numbers (~517 cm^{-1}) with a starting crystalline silicon powder material counterpart (~520 cm^{-1}) for samples (a) and (b), The value of FWHM of peaks and visible blue shift in peak positions increased with increasing thickness and this may be due to the strain results, which can be confirmed by XRD results. However, mechanical strain results in a change of this value. This shift increased with increase of the doping concentration due to a tensile strain in the film. The Raman results indicate that crystallization decreases slightly with increasing phosphoric acid concentration. The TO-mode is similar for all the samples. Thus, the Raman data indicate a decreasing strain with increasing thickness [15]. The microcrystalline and amorphous silicon material have different phonon modes with a broad peak starting from a Raman shift of 480 until 510 cm-1, corresponding to longitudinal optical (LO) and transverse acoustic (TA) modes These were not detected in our samples, indicating that our samples are polycrystalline phase [16].

3.2 XRD patterns of n-type silicon thin films printed on ITO-coated PET substrate

X-ray diffraction patterns of three Si films (a), (b) and (c) having thicknesses of 603, 611 and 619 nm respectively are shown in Fig 2. In all samples the dominant silicon peaks which have the highest intensities at 2□ are at 28.4°, 48° and 56° for Si (111), (220) and (313) respectively [17], while other peaks were detected only in sample (a) and we neglected these. The sharp peaks reveal that the deposited thin films were polycrystalline in nature. The effect of the thickness on the structure properties can be observed as changes in the peak intensities, but not in the peak positions. The significant line sharpness observed in the XRD patterns is attributed to both particle size and crystal defects, which indicate the good quality and nanostructure nature of the films. Furthermore, from Fig .2, it can be seen that the position of the peaks shifted towards lower diffraction angles with the increase of the doping concentration in the films and thickness, indicating changes in the lattice parameters due to the presence of the tensile strain in the host on incorporation of the dopant ions into the basic cell in the grown films. This may explain an increase in the crystallite size with increasing film thickness [18]. The crystallite size was calculated from the X-ray patterns using the Scherrer equation (1).

$$D = \frac{k\lambda}{\beta \cos\theta} \qquad (1)$$

Where β is the "full width at half maximum (FWHM)", and *k* is a constant equals to 0.94, λ is the incident x-ray wavelength (λ = 1.5406 Å) [19]

Lattice parameter *a*, which is equal to c in this case (cubic), can be calculated from equation (2).

$$d = \frac{a}{\sqrt{h^2 + k^2 + l^2}} \qquad (2)$$

The lattice constant calculated from this pattern has been found to be proportional with the thicknesses of the films and consistent with the standard value of a_o for bulk silicon. The determined lattice constants for the three thicknesses found that the values of the lattice parameters increase with the increasing thickness of the thin films [20].

The along a-axis, ε_a can be calculated from relations (3)

$$\varepsilon_a = \frac{a - a_0}{a_0} \qquad (3)$$

where a is the calculated lattice parameters and the standard and unstrained parameters values are $a_o = c_o = 5.434$Å for Si. The positive values for ε_a denote tensile strain while negative ones denote compressive strain. The value of strain decreases with increasing thickness [21]. The lattice parameter values a, in-plane strain (ε_a) and average crystal sizes determined for the samples are listed in Table 1.

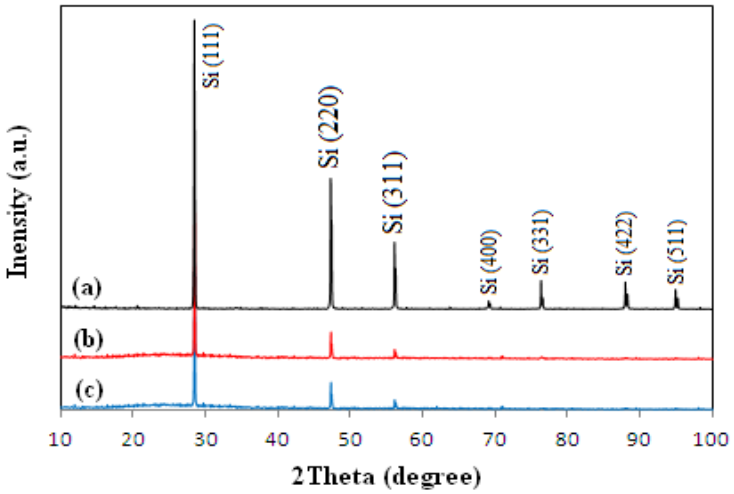

Figure 2. X-ray Diffraction patterns of n-Si films deposited on PET substrate with thicknesses of (a) 619 nm, (b) 611 and (c) 603 nm doped with phosphoric acid concentrations of 30 grams/liter, 20 grams/liter and 10 grams/liter respectively.

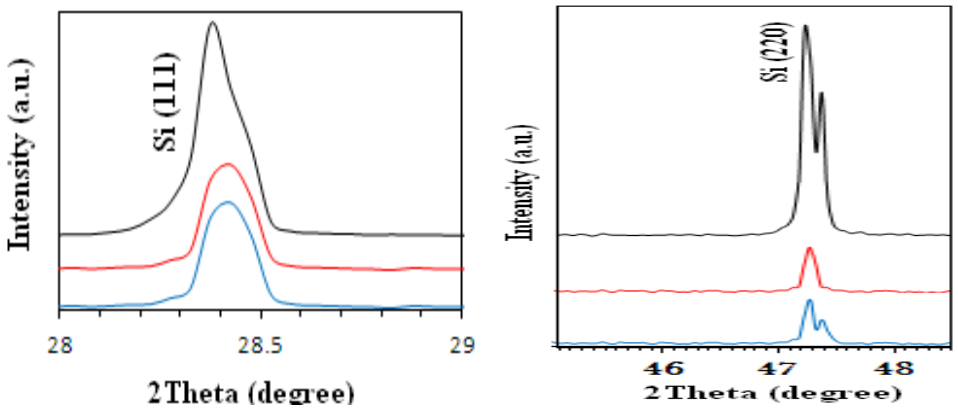

Figure 3. Shows X-ray Diffraction patterns of n-Si films plotted in figure 2. with more focusing for Si (111) and Si (220).

Table 1. Lattice parameters ($a = c$), in-plane strain (ε_a), out of plane strain (ε_c) and average crystal size determined of n-Si films deposited on PET substrate with thicknesses of (a) 619 nm, (b) 611 and (c) 603 nm doped with phosphoric acid concentrations of 30 grams/liter, 20 grams/liter and 10 grams/liter respectively.

Sample	phase	a (Å)	d (Å)	D (nm)	ε_a x10^{-3}
(a) 619 (nm)	Si (111)	5.4386	3.140	447.65	0.8465
	Si (220)	5.4337	1.9211	258.74	-0.0552
	Si (311)	5.4386	1.6398	254.09	0.84652
(b) 611 (nm)	Si (111)	5.4355	3.1382	434.86	0.27604
	Si (220)	5.4311	1.9202	226.45	-0.6337
	Si (311)	5.0977	1.5370	249.25	-61.8880
(c) 603 (nm)	Si (111)	5.4232	3.1311	428.75	-1.98749
	Si (220)	5.4029	1.9100	177.04	-5.72322
	Si (311)	4.9809	1.5018	173.07	-83.3824

3.3 SEM and EDX of n-type silicon thin films printed on ITO-coated PET

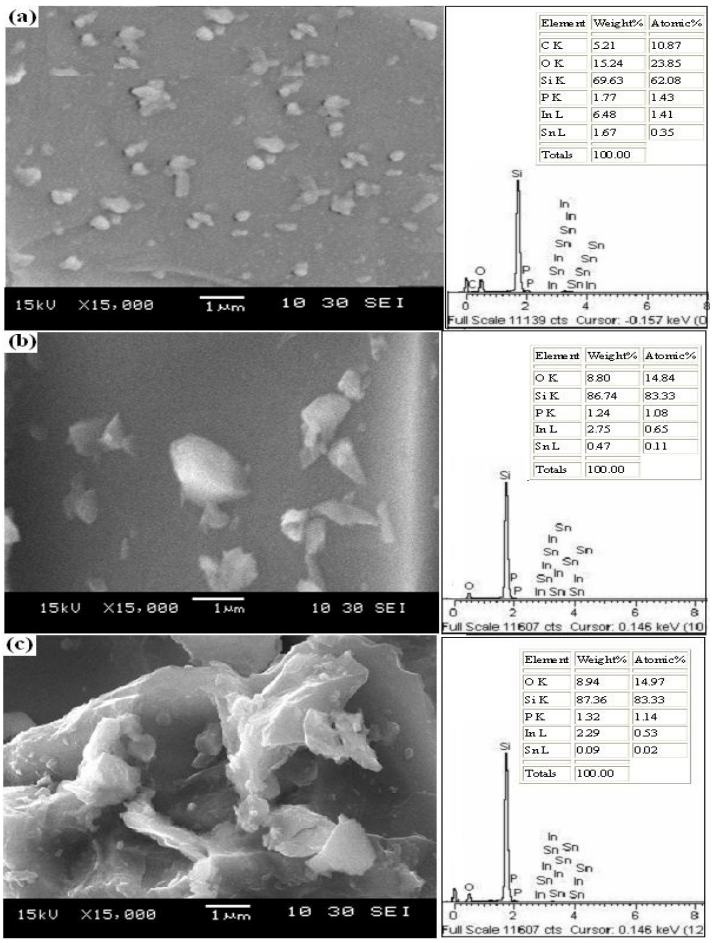

Figure 4. SEM images and EDX spectrums of n-Si films deposited on PET substrate with thicknesses of (a) 603 nm, (b) 611 and (c) 619 nm doped with phosphoric acid concentrations of 10 grams/liter, 20 grams/liter and 30 grams/liter respectively

SEM images of the printed n-Si layers in Fig.4 show clustering of the individual particles, which in turn cluster to form a self-similar structure that has different sizes increasing as the thickness and phosphoric acid concentration increased [22]. The Si layers were deposited as island increased with thickness and doping concentrations to the larger particles which were not perfectly continuous. Analysis of the chemical compositions was carried out by EDX. The entire films exhibit the same composition of elements and apparent chemical composition changes are shown in the attached tables. The peak of silicon increases with thickness while the amount of detected phosphorus changes randomly. The carbon spectrum in sample (a) corresponds to the PET substrate.

3.4 AFM images of n-type silicon thin films printed on ITO-coated PET

The surface morphology of Si thin films on ITO-coated PET substrates prepared with a screen-printing technique is characterized by AFM. Fig. 5 (a), (b) and (c) show 3D images of AFM of Si films with thicknesses of 603, 611 and 619 nm respectively, doped with phosphoric acid at concentrations of 0.1, 2.0 and 4.0 g/l respectively. The average and root mean square (RMS) were 211.4, 163.3 and 132 nm, for (a), (b) and (c) respectively. Although the printing conditions were fixed, the roughness of the printed films had large variations with small changes in thickness. This variation is not associated with the doping concentration but due to the hand printing and the limitation of heat treatments below the melting point of the PET substrate, which can also be affected by increasing stress on the film from increasing thickness [23].

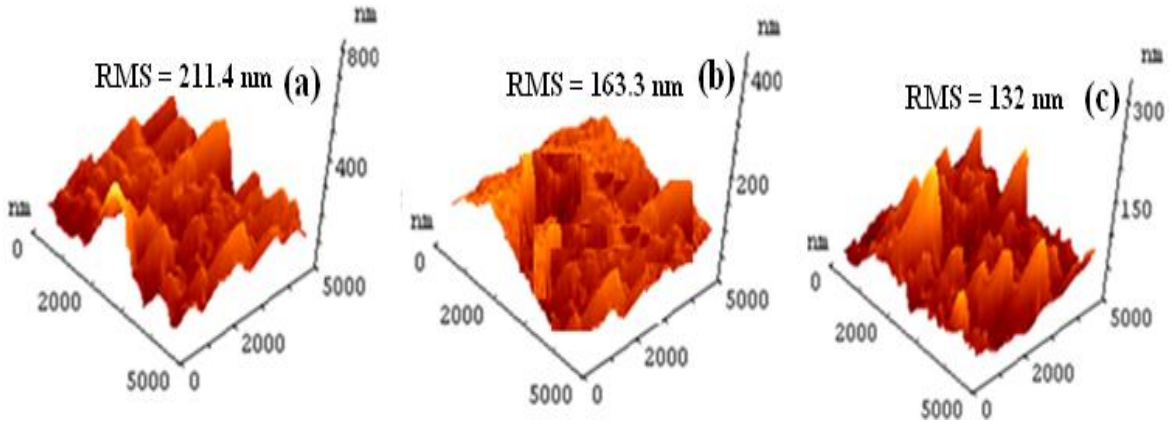

Figure 5. AFM images of n-Si films deposited on PET substrate with thicknesses of (a) 619 nm, (b) 611 and (c) 603 nm doped with phosphoric acid concentrations of 30 grams/liter, 20 grams/liter and 10 grams/liter respectively.

3.5 The optical properties of n-type silicon thin films printed on ITO-coated PET substrate

Fig. 6 is the transmittance spectra of n-Si thin films of different thicknesses from 603 nm to 619 nm in the wavelength range from 300 nm to 1100 nm. It shows that transmittance of Si thin films increases monotonically with the increase in wavelength, but decreases monotonically with the

increase in film thickness. The energy gap can be calculated by the maximum transmittance and the minimum absorbance, which are considered to be at the same wavelength, because the semiconductor reflectivity is constant at this wavelength [24]. So, E_g(T) is calculated from the derivative curve of transmittance.

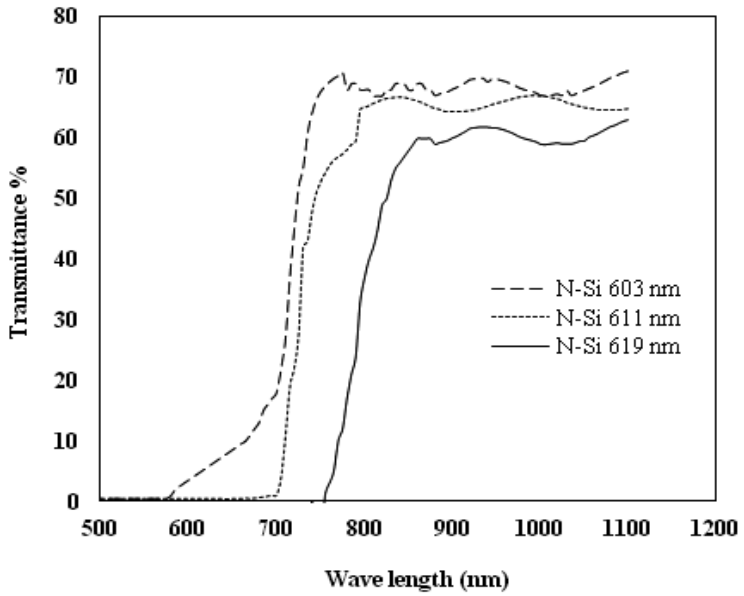

Figure 6. The optical transmittance spectrum of n-Si films deposited on PET substrate with thicknesses of 603 nm, 611 and 619 nm doped with phosphoric acid concentrations of 10 grams/liter, 20 grams/liter and 30 grams/liter respectively.

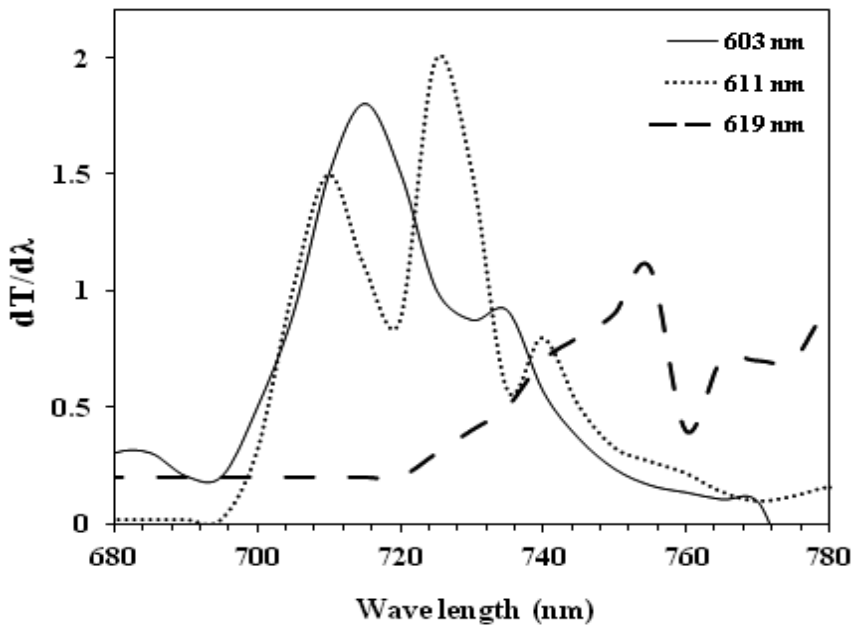

Figure 7. shows dt/dλ against the wavelength for transmittance spectrum n-Si films deposited on PET substrate with thicknesses of 603 nm, 611 and 619 nm doped with phosphoric acid concentrations of 10 grams/liter, 20 grams/liter and 30 grams/liter respectively.

These derivative curves in the wavelength range of interest are presented in Figu 7. The maximum peak value is associated with the optical band-gap energy E_g [25], which can be calculated from equation (4). From the optical spectra, the transmission edge shifts towards a longer wavelength with increasing thickness. This shift indicates a decrease of the optical band gap when the thickness increases, whereas thickness seems more important than concentration of phospric acid. The variations in the values of the optical band gap are summarized in Table 2.

$$E_g = \frac{hc}{\lambda_{max}} \qquad (4)$$

where h is the Planck constant, c is the light velocity and λ_{max} is the wavelength in the maximum of the derivative curve.

Table 2. The optical band gap values of n-Si films deposited on PET substrate with thicknesses of 603 nm, 611 and 619 nm doped with phosphoric acid concentrations of 10 grams/liter, 20 grams/liter and 30 grams/liter respectively.

Sample thickness (nm)	Wave length (nm)	Optical band gap (eV)
603.00	715	1.7343
611.00	725	1.7103
619.00	755	1.6424

3.6 The electrical properties of n-type silicon thin films printed on ITO-coated PET substrate

Poly-Si generally exhibits remarkably different electrical properties from c-Si because of the effect of grain boundaries (GBs) separated by thin amorphous zones or interfaces (grain boundaries) [26-28]. According to GB trapping theory [27], which are very widely accepted, free carriers in poly-Si are trapped at GBs and potential barriers are formed at GBs. The carrier transport in poly-Si is mainly dominated by the potential barriers, and the electrical conductivity can involve different mechanisms that depend on the structure of the samples, including their chemical nature [29]. For control of doping levels, n-Si films using three close values of the phosphoric acid concentrations are reported. The carrier concentration was obtained in n-Si films screen-printed at different doping concentrations. The Hall Effect measurement indicated that the carrier concentration decreased from 5.3×10^{16} to 6.49×10^{15}cm^{-3} as the phosphoric acid concentration decreased from 5.0 to 2.5 grams/liter, and when the distribution of the carrier concentration of Si films is scattered, it is difficult to determine the relationship between the carrier concentration and the phosphor content from the printed samples. On the other hand, there was a linear relationship between the film thickness and carrier concentration [30], which is in agreement with our results. The Hall mobility varies from 31 to 46 cm^2 V^{-1} s^{-1}. The films exhibit n-type semiconductor characteristics. Surface morphologies of films were needlelike

structures, which were clearly distinguished from polycrystalline structures to microcrystalline increase of doping concentrations. Structural changes caused by variation of the film composition affected the electrical resistivity and carrier concentrations. The dependence of resistivity and carrier Hall mobility on seeding layer thickness could be correlated with the differences in morphological changes observed by AFM and SEM. Thicker seeding layers give crystallized films with more gross defects, which are reflected in higher resistivity and lower mobility for both types of dopants. Since such gross defects were not observed in the films, it is possible that the morphological appearance and electrical performance of the Si films' structure would be further improved as the layer thickness decreases. This is suggested by the reduction of induced defects with the thinner seeding layer, and there should be an ultimate lower limit of the seeding layer thickness capable of inducing acceptable crystallization in the silicon layers. Phosphorus doping is cased defects can be involved to explain this increase of the defect density by doping. Also, the increase of the electrical resistivity in slightly doped poly-Si is due to doping-affected defects. The electrical properties of screen printed n-Si carried out by Hall Effect measurement are listed in Table 3.

Table 3. The electrical properties of n-Si films deposited on PET substrate with thicknesses of (a) 603 nm, (b) 611 and (c) 619 nm doped with phosphoric acid concentrations of 10 grams/liter, 20 grams/liter and 30 grams/liter respectively.

Sample Thickness (nm)	Sheet resistant Rs(Ω /square)	Resistivity ρ (Ω-cm)	carrier concentration N (cm^{-3})	Hall Coefficient (m^2/C)	Hall mobility μ_H (cm^2/v-s)
(a) 603.00	466.9	281.54	6.49×10^{15}	-3.71×10^{-5}	7.98
(b) 611.00	580.3	354.56	2.11×10^{16}	-7.05×10^{-6}	1.85
(c) 619.00	655.2	405.57	5.30×10^{16}	-2.43×10^{-6}	0.83

4. CONCLUSIONS

Various characterization tools have been used to investigate the structural, optical and electrical properties of n-type silicon thin film with thicknesses of 611.0 ± 8.00 nm and carrier concentration of 10^{15} cm^3 deposited on ITO coated PET substrate by using a screen-printing technique and the effect of phosphoric acid doping concentration on the properties of n-type silicon thin films has been studied.

The results showed that the Si films had polycrystalline structure with crystal size about 447-429 nm and high roughness surface with rot main square about 132-212 nm. The Si films were exhibited optical transmittance of 74% in UV-Visible rang for thickness of 603 nm doped by phosphoric acid concentrations of 10 grams/liter. The optical transmittance is decrease with doping concentration increasing. Phosphorus doping is cased defects can be involved to explain this increase of the defect density by doping. Also, the increase of the electrical resistivity in slightly doped poly-Si is due to doping-affected defects.

ACKNOWLEDGMENTS
This work was supported by the Nano-optoelectronics Research Laboratory, School of Physics: Universiti Sains Malaysia and financial supported under grant number: 203/PSF/6721001.

References

1. G. seeg , *Mater. Res. Soc. Symp. Proc. Vol*. 377 (1997) and Vol. 468 (1998)
2. J.Esher, D.Redfield , *Appl. Phys. Lett*. 25, (1974) 702.
3. K.Gosh , C. Fishman, T.Feng , *J. Appl. Phys*,51(1980) 446–454.
4. M.Green , Silicon Solar Cells, University of New South Wales, Sydney, Australia (1995).
5. E. Yablonovitch , G.Cody , *IEEE ED* ,29(1982) 300.
6. F.A. Nour El-Dien, G.G. Mohamed, E.Y.Z. Frag, M.E. Mohamed, *Int. J. Electrochem. Sci*, 7 (2012) 10266 – 10281.
7. M. Harting, J. Zhang, D. R. Gamota, D. T. Britton , *Appl. Phys. Lett*,94 (2009) 193509.
8. Z. Bao, Y. Feng, A. Dodabalapur, V. R. Raju, A. J. Lovinger, *Chem. Mater* , 9 (1997)1299–1301.
9. M. Guerin, A. Daami, S. Jacob, E. Bergeret, E. Benevent, P. Pannier, R. Coppard, *IEEE Trans. Electron Devices* ,58 (2011) 3587–3593.
10. J. Szlufcik, F. Duerinckx, J. Horzel, E. Van Kerschaver, H. Dekkers, S. D.Wolf, P. Choulat, C.Allebe, J. Nijs, *Solar Energy Materials & Solar Cells* ,74 (2002) 155–163.
11. D. Bouhafs, A. Moussi, M. Boumaour , S.E.K. Abaïdia, L. Mahiou . *Thin Solid Films*, 2006.510(1): p. 325-328.
12. Stevens, G.D. and J.S. Reynolds, Phosphorous doping a semiconductor particle. 1999, USA. Google Patents.
13. Kwon, T., et al., T.Y. Kwon, D.H. Yang, M.K. Ju, W.W. Jung, S.Y. Kim, Y.W. Lee, D.Y. Gong, *Solar energy materials and solar cells*, 5(1) (2011. 9) 14-17.
14. Sano, Naoki; Maki, Masato; Andoh, Nobuyuki; Sameshima, Toshiyuki.*Japanese journal of applied physics*, 46 (2007) 1254.
15. F .Cerdeira, W. Holzapfel, D. Bäuerle, *Physical Review* B, 11(3) 1975. 118.
16. H.Richter, Z. Wang, L. Ley, *Solid State Communications*, 39(5) (1981) 625-629.
17. M.Moreno, R. Boubekri, P. R.Cabarrocas, *Solar energy materials and solar cells*, 100 (2012) 16-20.
18. M.El-Hagary, M. Emam-Ismail, E.R. Shaaban, A. Al-Rashidi, S. Althoyaib . *Materials Chemistry and Physics*, 132(2) (2012) 581.
19. S. Veprek, F.A. Sarrot, Z. Iqbal , *Phys. Rev*, 36 (1987) 3344.
20. J.Kühnle, R.B. Bergmann, *J.H.Journal of crystal growth*,173(1) (1997)62-68
21. C.Smit, van Swaaij, R. A. C. M. M. Donker, H. Petit, A. M. H. N. Kessels, W. M. M. ; van de Sanden, *Journal of Applied Physics*,94 (2003) 3582 - 3588
22. D.Britton, M. Härting, *Pure and applied chemistry*, 78(9) (2006) 1723-1740.
23. W.H.Yang, D.J. Srolovitz, *Journal of the Mechanics and Physics of Solids*, 42(10) (1994) 1551-1574.
24. N.Veissid, C.Y. An, A. F.Silva, J.I. P.Souza. *Materials Research*, 2(4) (1999) 279-281.
25. S.Ferreira ,N. Veissid, C. Y. An, I.Pepe, B. Oliveira, N. B. Silva, *Applied Physics Letters*, 69(13) (1996) 1930-1932.
26. K.Maydell, S. Brehme, N.H. Nickel, W. Fuhs. *Thin Solid Films*, 487(1) (2005) 93-96.
27. M, Taniguchi, M, Hirose, Y,Osaka, S,Hasegawa, T.Shimizu, *Jpn. J. Appl. Phys*, 19(4) (1980). 665-673.
28. M.Mandurah M, K. Saraswat, T. Kamins, *Journal of The Electrochemical Society*,126(1979) 1019.

29. M. Zaghdoudi, M.M. Abdelkrim, M. Fathallah, T. Mohammed-Brahim, F. Le Bihan. *Materials Science forum* (480-481) (2005) 305-308.
30. B.Y. Yoo,C.K. Huang, J.R. Lim, J. Herman, M.A. Ryan, J.-P. Fleurial, N.V. Myung *Electrochimica acta*, 50(22)(2005) 4371-4377.